Food and Bioprocess Technology (2026) 19:220
https://doi.org/10.1007/s11947-026-04310-4

RESEARCH

Advanced Bacteriophage-Loaded Nanofiber Coatings for Active Food Packaging

Fernanda Coelho[1,2] · Victor Gomes Lauriano de Souza[2,3,4] · Pedro Miguel Silva[2] · Lorenzo Pastrana[2] · Sanna Sillankorva[2] · Valtencir Zucolotto[1]

Received: 24 September 2025 / Accepted: 6 March 2026

Abstract

The food industry faces significant challenges from microbial contamination, particularly by *Salmonella*, a leading cause of foodborne illnesses. Bacteriophages offer a promising biocontrol strategy due to their host specificity, safety, and environmental sustainability, but their practical application is limited by stability issues. This study presents a scalable approach to develop phage-functionalized antimicrobial packaging by electrospinning Felix O1 phage-loaded nanofibers composed of a dual hydrophilic polymer blend of sodium alginate and hydroxypropyl methylcellulose (HPMC) directly onto food-grade substrates (parchment paper and polystyrene). Parchment paper coatings achieved higher phage loading ($\approx 10^9$ PFU/mL) compared to polystyrene ($\approx 10^8$ PFU/mL), with thicknesses of 46.5 ± 0.24 µm and 59.7 ± 0.94 µm, respectively. Contact angles decreased from 107.6 to 45.7° on parchment and from 91.4 to 70.1° on polystyrene, indicating increased hydrophilicity, while water vapor transmission remained largely unchanged. Phage release exhibited a burst pattern, reaching ~ 100% release from parchment and films within 20 min, and 93.5% from polystyrene in 40 min. Antibacterial testing against *Salmonella* enteritidis demonstrated substrate-dependent efficacy. The electrospun films achieved the highest antimicrobial performance, with a 2.95 log reduction in bacterial counts, followed by coated parchment paper (2.05 log reduction), whereas polystyrene coatings exhibited a comparatively lower reduction of 0.76 log. These results were consistent with inhibition halo diameters of 24–25 mm for films, 16–17 mm for coated parchment, and slightly lower activity for polystyrene coatings. FTIR and mechanical analyses confirmed polymer deposition and improved tensile strength, particularly on parchment. These findings demonstrate that substrate surface properties strongly influence nanofiber deposition, phage incorporation, release kinetics, and antimicrobial efficacy. This work is the first to integrate bacteriophages into a dual-polymer electrospun nanofiber matrix directly applied to real-world food packaging, providing a practical and scalable strategy for active antimicrobial packaging.

Keywords Bacteriophages · Electrospinning · Antimicrobial coatings · Nanofiber adhesion

Introduction

The food industry is constantly evolving to enhance product quality and safety. A persistent and critical challenge remains microbial contamination, which can lead to food spoilage and the transmission of foodborne diseases (Costa et al., 2021). Among the pathogens implicated, *Salmonella* stands out not only for its global health burden but also for the significant economic impact arising from hospitalizations, food recalls, and productivity losses. In the USA alone, *Salmonella* is estimated to cause approximately 1.35 million infections annually, 26,500 hospitalizations, and 420 deaths (CDC, 2023), while in Europe it remains among the most frequently reported zoonotic diseases despite extensive control programs (EFSA, 2024). These

✉ Fernanda Coelho
fernanda.coelho1408@gmail.com

✉ Sanna Sillankorva
sanna.sillankorva@inl.int

1 Nanomedicine and Nanotoxicology Group (Gnano), São Carlos Institute of Physics, University of São Paulo, São Carlos, São Paulo, Brazil

2 International Iberian Nanotechnology Laboratory, Braga, Portugal

3 Departamento de Química, MEtRICs/CubicB, NOVA School of Science and Technology, FCT NOVA, Universidade Nova de Lisboa, Campus de Caparica, 2829-516 Caparica, Portugal

4 GeoBioTe, Department of Earth Sciences, NOVA School of Science and Technology, NOVA University Lisbon, Campus de Caparica, 2829-516, Caparica, Portugal

Published online: 16 March 2026

data underline the urgent need for targeted antimicrobial interventions that go beyond conventional preservation strategies.

Concurrently, consumer demand is shifting toward minimally processed, natural, and fresh-like foods, placing stricter requirements on packaging systems to ensure extended shelf life, minimal chemical residues, and preservation of sensory quality (Zanetti et al., 2018). This paradigm shift has accelerated the development of advanced packaging technologies, including edible films and coatings, smart packaging, biodegradable materials, and particularly active packaging systems that interact dynamically with food products to enhance safety and stability (Ghaani et al., 2016).

Among emerging antimicrobial strategies, bacteriophage-based biocontrol has gained considerable attention in the agro-food sector. Lytic bacteriophages exhibit high host specificity, selectively targeting pathogenic bacteria without disrupting beneficial microbiota or eukaryotic cells (Becerril et al., 2020; Alves et al., 2019). They are relatively inexpensive to produce, adaptable to different targets, and increasingly recognized as safe biological control agents. Recent reviews have positioned phages as "natural antimicrobial bioadditives" for food packaging applications, highlighting their specificity and regulatory potential (Wagh et al., 2023).

Despite these advantages, integrating bacteriophages into packaging matrices remains challenging due to stability limitations during processing and storage, potential loss of infectivity, and difficulties in achieving controlled and effective release under real food-contact conditions (Huang & Nitin, 2019). To address these constraints, nanostructured delivery systems have emerged as promising platforms. In particular, electrospun nanofibers offer high surface-area-to-volume ratios, interconnected porosity, and tunable physicochemical properties, making them highly suitable for the immobilization and controlled release of antimicrobial agents (Greiner & Wendorff, 2007). Recent advances have demonstrated the versatility of electrospun nanofibrous systems in food packaging, highlighting their potential for improved barrier properties, active compound delivery, and scalable fabrication routes (Ashraf et al., 2025; Mathew et al., 2025; Zhang et al., 2023). These studies reinforce the growing relevance of nanofibers as next-generation materials for active packaging. However, most reported approaches rely on free-standing nanofibrous mats or model membranes, with limited exploration of their direct integration onto commercially relevant food-grade substrates. This gap significantly limits practical translation, as substrate surface properties critically influence nanofiber adhesion, bioactive incorporation, release behavior, and antimicrobial performance.

This work is the first to demonstrate the direct electrospinning of a sodium alginate–HPMC dual-polymer nanofiber coating loaded with Felix O1 bacteriophage onto conventional food-grade packaging substrates, namely parchment paper and polystyrene. By combining a hydrophilic dual-polymer system optimized for phage incorporation with in situ deposition onto industrially relevant materials, we establish a scalable strategy that bridges laboratory-scale electrospinning with real-world packaging applications. We systematically evaluate how substrate surface characteristics, such as surface energy and morphology, affect nanofiber formation, phage loading, release kinetics, and antimicrobial efficacy. Through this integrative approach, the present study advances active packaging technology by directly linking material engineering parameters with biological performance, thereby offering a practical pathway toward phage-functionalized commercial packaging solutions.

Materials and Methods

Materials

Alginic acid sodium salt, magnesium nitrate, sodium chloride, and hydroxypropyl methylcellulose (HPMC) were acquired from Sigma-Aldrich (Portugal). Glycerol 99.5% (v/v) was purchased from Alfa Aesar (USA), Tris base and polyethylene glycol (PEG) 8000 were purchased from Fisher BioReagents™ (USA), and calcium chloride and MgSO4 from Panreac Applichem (Spain). Tryptic Soy Broth (TSB): Corning® (USA), Tryptic Soy Agar (TSA): Hardy Diagnostics, Criterion™ line (USA).

Bacteriophage Felix O1 was kindly provided by Sanna Sillankorva (Portugal), and the International Iberian Nanotechnology Laboratory (INL) provided the *S. Enteritidis* (SE 269) used in this work.

Bacteria

Salmonella enteritidis 269 (SE 269) (Invitrogen, ThermoFisher Scientific) was used as host for phage isolation. This bacterium was grown at 37 °C in liquid or solid TSB medium (TSB + 1.5% (w/v) of agar).

Phage Propagation and Titration

Bacteriophage propagation was carried out using the plate lysis and elution technique, adapted from the classical protocol of Sambrook and Russell (2001). Quantification of phage concentration was performed following the plaque assay method described by Adams (1959), with results expressed in plaque-forming units per milliliter (PFU/mL).

Fabrication of Antimicrobial Coatings on Parchment Paper and Polystyrene Substrates Using Electrospun Nanofibers

Preparation of Alginate + HPMC Solution with Bacteriophage Felix O1

A 2.25% (w/v) HPMC solution was prepared in distilled water under continuous stirring at room temperature for

18 h. Sodium alginate was then added to a final concentration of 1.5% (v/v), resulting in a solution containing 1.5% HPMC and 0.5% sodium alginate, which was stirred at 250 rpm. Phage Felix 01 was then incorporated to achieve a final concentration of approximately 10^{10} PFU/mL in the solution, followed by stirring for 30 min at room temperature.

Antimicrobial Parchment Paper and Polystyrene Substrates Production Using Electrospun Nanofibers

For the electrospinning process, the HPMC and sodium alginate solution containing Felix O1 at a titer of 10^{10} PFU/mL was loaded into a 10-mL plastic syringe fitted with a stainless steel needle (∅ 1.07 mm) and electrospun directly onto 25 cm^2 parchment paper and polystyrene substrates for 2 h. The process was carried out at 20 kV and a flow rate of 1.0 mL/h, with a needle-to-collector distance of 20 cm. All experiments were performed at room temperature (23 °C) using a NanoNC eS-robot electrospinning apparatus (NanoNC, Korea). These electrospinning parameters—voltage, flow rate, and needle-to-collector distance—were optimized through multiple trials to ensure the formation of uniform nanofibers without beads, with an average diameter of approximately 100 nm, capable of incorporating the bacteriophage. During optimization, voltage values between 9.5 and 21 kV, flow rates ranging from 0.6 to 1.0 mL/h, and needle-to-collector distances between 16 and 20 cm were tested, allowing the selection of conditions that provided the most stable jet formation and consistent fiber morphology. For bacteriophage analysis, the parchment paper and polystyrene substrates were stored at 4 °C for further experiments.

Characterization of Nanofiber

Scanning Electron Microscopy (SEM)

The morphology and surface characteristics of the nanofibers and coatings were analyzed using scanning electron microscopy (Quanta FEG 650, FEI, USA). Samples were sputter-coated with a thin layer of gold using a Leica EM ACE200 coater. Images were acquired at varying magnifications using an accelerating voltage of 10 kV to observe fiber uniformity and structure. Nanofiber diameters were measured using ImageJ software (National Institutes of Health, USA), based on manually selected fibers, and the diameter distribution and statistical analysis were subsequently performed using OriginPro 2023 (OriginLab Corporation, USA). A total of 100 individual nanofibers were measured for each sample to ensure representative morphological characterization.

Fourier Transform Infrared Spectroscopy (FTIR)

Chemical structure analysis was performed using a Bruker Alpha II FTIR spectrometer (VERTEX 80/80v, Bruker, USA), operating in the ATR (Attenuated Total Reflectance) mode. Spectra were recorded over the range of 500 to 4000 cm^{-1} at a resolution of 4 cm^{-1}. All spectra were normalized on a scale from 0 to 1 to allow for comparative analysis.

Thickness, Grammage, and COBB Test

Sample thickness was determined at five different points using a precision digital micrometer (Schut, Netherlands; ± 0.001 mm accuracy). Grammage was calculated according to the ASTM D646-96 methodology (American Society for Testing and Materials [ASTM], 2007) by weighing each sample with a semi-analytical balance (Ohaus ARD110, USA) and applying Eq. (1):

$$G = \frac{M}{A} \tag{1}$$

Water absorption capacity (WAC_Cobb) was assessed using the TAPPI T 441 om-98 method. Pre-weighed square samples (12.5 × 12.5 cm) were fixed in a COBB test cell (Techlabsystems, Spain), exposed to 100 mL of water for 60 s, and then blotted with absorbent paper using a 10-kg roller. The final mass was recorded, and water absorption was calculated using Eq. (2):

$$\mathrm{WAC_{Cobb}} = \frac{(M_f - M_i)}{0.01} \tag{2}$$

Opacity and Color

Opacity was calculated following the Hunter Lab method, as the ratio between the sample's *Y*-value reflectance on a black background (Yb) and on a white background (Yw), expressed in percentage (Eq. 3):

$$\mathrm{Opacity} = \left(\frac{\mathrm{Yb}}{\mathrm{Yw}}\right) \times 100 \tag{3}$$

Color parameters (L^*, a^*, b^*) were recorded using a PCE-CSM7 colorimeter. Chroma (C^*) and hue angle ($h°$) were calculated using Eqs. (4) and (5):

$$C^* = \left(\frac{a^2}{b^2}\right) \times 0.5 \tag{4}$$

$$h^\circ = \arctan\left(\frac{b^*}{a^*}\right) \tag{5}$$

Surface Hydrophobicity and Water Vapor Permeability (WVP)

Hydrophobicity was assessed using the sessile drop method, as outlined by Espitia et al. (2014). A 5-µL droplet of ultrapure water was placed on the surface of each film or coating using a Hamilton precision syringe. Contact angles were measured after 60 s using a goniometer (OCA 20, DataPhysics, Germany), and the Laplace-Young model was applied to fit the droplet profile. Each sample was measured in triplicate.

WVP was determined using the gravimetric desiccant method ASTM E96/E96M (American Society for Testing and Materials [ASTM], 2013). Film samples were sealed over Payne permeability cups (35 mm diameter) containing 10 g of anhydrous $CaCl_2$ (0% RH) and placed inside a desiccator maintained at 54% RH (20 °C) with saturated magnesium nitrate. A fan ensured uniform humidity. The mass gain of the cups was monitored over time, and the WVP ($g \cdot m^{-1} \cdot s^{-1} \cdot Pa^{-1}$) was calculated using Eq. (6):

$$\mathrm{WVP} = \frac{(\mathrm{WVTR} \times L)}{\mathrm{DP}} \tag{6}$$

Mechanical Properties Mechanical performance of the films and coatings was evaluated using a Universal Testing Machine (AGX-V 10 kN, Shimadzu, Japan) equipped with a 500-N load cell. The tests were conducted following ASTM D882–10 (American Society for Testing and Materials [ASTM], 2010) guidelines, with slight modifications. Rectangular samples (50 mm × 20 mm) were fixed between grips set 40 mm apart and stretched at a constant rate of 50 mm/min until rupture. The tensile strength (TS), elongation at break (EB), and Young's modulus (YM) were calculated based on the force and deformation data collected. Each sample was analyzed in at least six replicates.

The TS and EB were calculated using the following equations:

$$\mathrm{TSB(MPa)} = \frac{\text{maximum load (N)}}{\text{initial cross} - \text{sectional area } (m^2)} \tag{7}$$

$$\mathrm{EB}(\%) = \frac{\text{final length at the point of sample rupture (mm)}}{\text{Initial length of the specimen (mm)}} \tag{8}$$

YM was determined from the slope of the linear region of the stress–strain curve.

Loading Efficiency and Release

The loading efficiency and release of phages in alginate + HPMC solution films and coatings were evaluated using PFU/mL measurements. For *Salmonella*, theoretical loading was determined to be 2.24×10^{10} PFU/mL for films and 5.6×10^{8} PFU/mL for coatings. To assess the phage release profile from alginate + HPMC solution films and coatings, round samples (1 cm diameter) were placed in 500 µL of SM buffer (50 M Tris–HCl, 100 mM NaCl, 8 mM $MgSO_4$, 0.01% gelatin, pH 7.5) under continuous agitation at room temperature (22 °C). Samples were collected at designated time points to evaluate phage release. The quantity of released phage particles was determined by counting plaque-forming units (PFU).

Antimicrobial Activity

The antimicrobial activity of phage-coated substrates was evaluated according to the ISO 22196 standard. Phage-coated samples and control samples were prepared, using *Salmonella* as the test organisms, with cultures adjusted to approximately 10^5 CFU/mL. Each sample was inoculated with the bacterial suspension and incubated at 37 °C for 24 h. After incubation, surviving bacterial counts were determined using serial dilution and selective agar plating. Antimicrobial efficacy was assessed by comparing the viable counts from phage-coated samples to those from control samples, with reductions expressed as log reductions. All experiments were performed in triplicate.

Results and Discussion

Characterization of Nanofibers

Morphology Analysis

Figure 1 shows the surface of electrospun nanofibers deposited on parchment paper and polystyrene, along with the control surfaces of the materials. Predominantly continuous nanofibers were formed on both materials, with a noticeably higher fiber density on parchment paper; however, bead formation was also observed, especially on polystyrene. Figure 1 also presents the size distribution of the nanofibers on the material surfaces. The average nanofiber diameter was 115.4 nm for parchment paper and 150.9 nm for polystyrene coatings.

Electrospun nanofibers tend to deposit more efficiently on parchment paper than on polystyrene due to the difference in surface energy and texture between the two materials. Parchment paper has a more porous, rougher, and hydrophilic surface compared to the smooth, non-polar, and hydrophobic surface of polystyrene (Samyn, 2013). The porosity and increased surface area of parchment paper provide more sites for the nanofibers to adhere to, while the low surface energy of polystyrene creates a weaker interaction with the fibers, leading to less efficient deposition

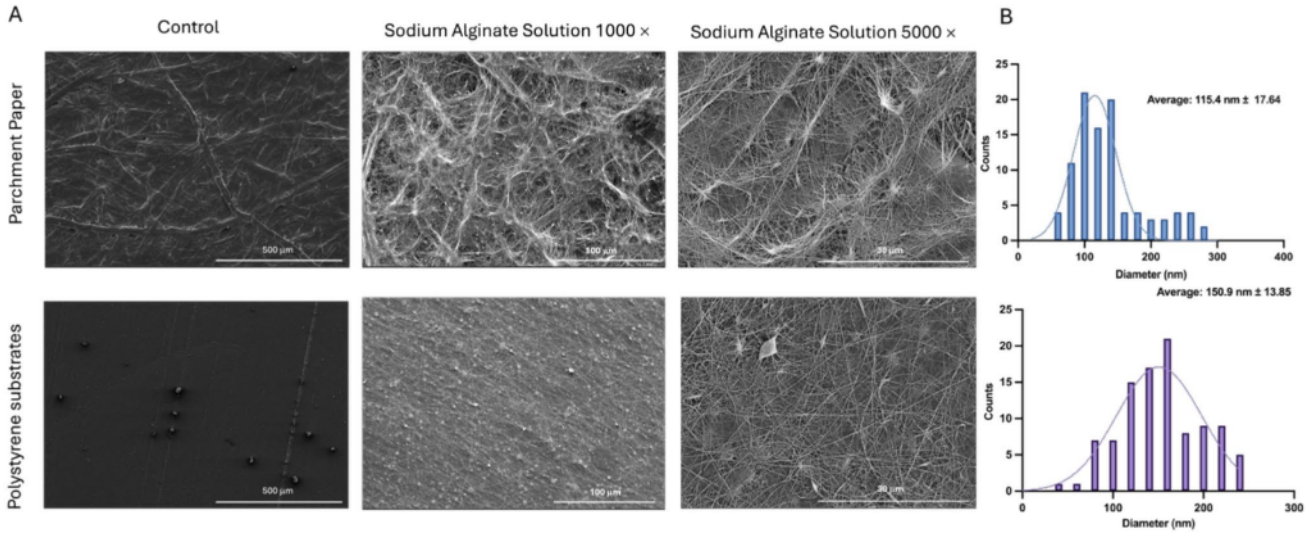

Fig. 1 (**A**) SEM images of nanofibers obtained at 1000× and 5000× magnification. (**B**) The graphs represent the estimation of nanofiber size distribution

(Choi et al., 2017). Consequently, electrospun nanofibers are more likely to adhere to and accumulate on parchment paper, enhancing their deposition density. This stronger interaction between the charged jet and the higher-energy, more hydrophilic parchment paper surface also contributes to greater jet stretching during the flight and deposition phases, resulting in thinner fibers. In contrast, the low-energy hydrophobic polystyrene surface leads to reduced electrostatic attraction and less jet elongation, which is consistent with the larger fiber diameters observed on this substrate (Xue et al., 2019).

Chemical Structures

The FTIR technique was used to analyze the composition and surface characteristics of the produced coatings. The infrared spectra, shown in Fig. 2 (A, B), highlight the main peaks associated with sodium alginate, marked in red and blue, which are present in both coated substrates.

However, these peaks are more pronounced in the parchment paper compared to the polystyrene, a fact previously explained by the higher deposition of nanofibers on the parchment paper. These peaks correspond to functional groups typical of alginate, including hydroxyl (-OH) and carboxylate (-COO) groups, which are typically observed around 3200–3600 cm^{-1} and 1400–1600 cm^{-1}, respectively. (Marangoni Júnior et al., 2021). The absence of characteristic bands corresponding to hydroxyl (3200–3600 cm^{-1}) and carboxylate (1400–1600 cm^{-1}) groups in the samples deposited on polystyrene can be attributed to the low affinity of the hydrophobic surface for the biopolymers used. In contrast, the hydrophilic and porous nature of parchment paper promoted the deposition of the nanocomposites, as evidenced by the higher intensity of these bands (Samyn, 2013). Signals attributable to phage proteins (amide I and II) were mainly observed in the spectra from paper-based samples, indicating a comparatively lower immobilization efficiency of phages on the polystyrene surface, which remains a key consideration when applying such systems to non-polar substrates (Xie et al., 2022).

Thickness, Grammage, and COBB Test

The evaluation of physical properties such as thickness, grammage, and water absorption is essential to understand the impact of coating processes on substrate performance. These parameters are particularly relevant for assessing the uniformity of deposition and potential functional enhancements, such as improved barrier properties.

The uncoated control samples were used solely as material references, and grammage was measured only after coating application. Since the objective of the study was to compare coated samples produced on the same base paper or polystyrene substrates, grammage values for the uncoated controls are not applicable and are therefore reported as N/A.

According to the data presented in Table 1, the application of polymeric coatings on both parchment paper and polystyrene substrates led to a measurable increase in thickness and grammage, confirming successful deposition. For parchment paper, the average thickness increased from 40.17 ± 2.59 µm in the control to 46.50 ± 0.24 µm in the phage-containing formulation, representing a 15.75% increase. A similar trend was observed in the grammage values, which rose from undetectable levels in the control to 0.62 ± 0.016 g/m^2 and 0.58 ± 0.026 g/m^2 for coatings without

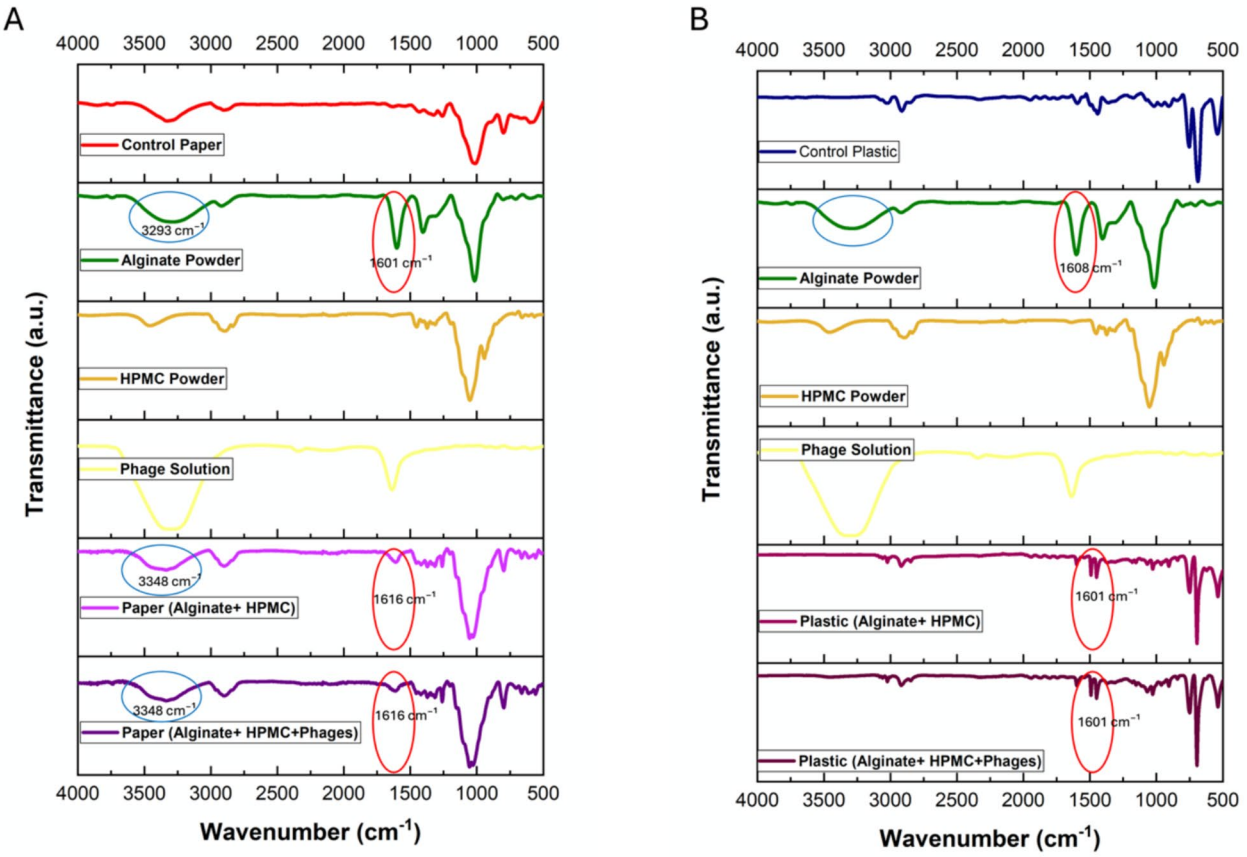

Fig. 2 FTIR spectra comparing control substrates (plastic and paper), alginate powder, HPMC powder, phage solution, and alginate-HPMC-based coatings on different substrates: **A** coatings on paper and **B** coatings on plastic. Key characteristic peaks of alginate and HPMC are highlighted in red and blue circles, including carboxylate groups (-COO) at 1400–1600 cm^{-1} and the peak near 3500 cm^{-1} corresponding to the O = H stretching bands

Table 1 Thickness, grammage, and water absorption (COBB Test) values for the different material matrices

Matrix		Thickness (µm)	Grammage (g/m^2)	COBB Test (g/m^2)
Parchment paper	Control	40.17 ± 2.59^{A}	N/A	11.73 ± 0.02^{A}
	Without phages	45.50 ± 1.65^{A}	0.62 ± 0.016^{A}	14.23 ± 0.54^{A}
	With phages	46.50 ± 0.24^{A}	0.58 ± 0.026^{A}	16.64 ± 0.40^{A}
Polystyrene	Control	57.67 ± 2.36^{A}	N/A	0.14 ± 0.03^{A}
	Without phages	59.83 ± 0.24^{A}	0.24 ± 0.056^{A}	0.17 ± 0.04^{A}
	With phages	59.67 ± 0.94^{A}	0.21 ± 0.024^{A}	0.18 ± 0.10^{A}

Superscript letters (A, B): Within each respective material group, values in the same column not sharing upper case superscript letters indicate statistically significant differences between each other ($p < 0.05$). *N/A* not applicable.

and with phages, respectively. This increase in mass and thickness indicates that the coating was effectively deposited on the substrate surface.

For polystyrene, although the increase in thickness was more modest—from 57.67 ± 2.36 µm to 59.67 ± 0.94 µm (3.47%)—the increase in grammage and slight variation in COBB values also indicate the presence of a coating layer, albeit thinner. This difference may be attributed to the intrinsic hydrophobic and smooth nature of polystyrene, which reduces surface wettability and adhesion efficiency compared to parchment paper.

Similar findings were reported by Coelho et al. (2025), who observed increased thickness in both substrates after applying alginate-based coatings using ultrasonic spray. In

Table 2 Chroma, hue (°), and opacity (mm^{-1}) values for the different material matrices

Matrix		*l*	*a*	*b*	Chroma	Hue (°)	Opacity (mm^{-1})
Parchment paper	Control	$96,36 \pm 0.01^{A}$	$0,42 \pm 0.02^{A}$	$1,39 \pm 0.02^{A}$	1.47 ± 0.03^{A}	73.22 ± 0.05^{A}	32.48 ± 1.55^{A}
	Without phages	96.28 ± 0.02^{A}	0.39 ± 0.01^{A}	1.48 ± 0.01^{A}	1.48 ± 0.02^{A}	74.55 ± 0.84^{A}	33.87 ± 1.56^{A}
	With phages	96.29 ± 0.02^{A}	0.38 ± 0.02^{A}	1.50 ± 0.03^{A}	1.49 ± 0.01^{A}	75.08 ± 0.33^{A}	35.16 ± 3.65^{A}
Polystyrene	Control	96.04 ± 0.03^{A}	0.28 ± 0.02^{A}	1.07 ± 0.02^{A}	1.08 ± 0.03^{A}	75.32 ± 0.02^{A}	16.84 ± 0.31^{A}
	Without phages	96.07 ± 0.04^{A}	0.21 ± 0.03^{A}	1.05 ± 0.01^{A}	1.07 ± 0.01^{A}	78.20 ± 0.27^{AB}	16.00 ± 0.62^{A}
	With phages	96.05 ± 0.03^{A}	0.27 ± 0.02^{A}	1.07 ± 0.03^{A}	1.08 ± 0.02^{A}	78.53 ± 0.21^{B}	16.34 ± 0.21^{A}

Superscript letters (A, B): Within each respective material group, values in the same column not sharing upper case superscript letters indicate statistically significant differences between each other ($p < 0.05$).

their study, parchment paper exhibited a 27.5% increase in thickness and polystyrene a 19% increase, values higher than those obtained in the present study. The differences may result from variations in polymer concentration, coating method, or deposition time, but overall, both studies support the efficiency of biopolymer-based coating strategies on different packaging substrates.

Opacity and Color

According to the study by Blachowicz and Ehrmann (2023), the opacity of nanofibers is directly linked to the scattering and absorption of light. Due to their nanometric diameter and highly porous structure, nanofibers can exhibit significant light scattering, which increases the material's opacity. This characteristic is influenced by factors such as fiber diameter, fiber density and overlap, and the refractive index of the polymer. The color of electrospun nanofibers is determined by various optical and structural factors, including selective light absorption and interference effects within the fibrous structure. Key factors influencing color include the nature of the polymer and additives, the morphology of the fibers, and the presence of pigments or nanoparticles.

To evaluate the visual impact of the coatings on the materials, colorimetric parameters (chroma and hue) and opacity were measured, as presented in Table 2. These properties are essential for understanding how the coatings affect the aesthetic and functional aspects of the substrates, especially in applications where visual transparency or light protection is relevant.

The present study showed no statistically significant differences in chroma values within each substrate group, indicating that the coatings formulated with sodium alginate and HPMC did not substantially alter the color saturation of the materials ($p > 0.05$). Similarly, hue values remained relatively stable, suggesting that the overall color tone of the substrates was not perceptibly affected by the presence of phages or the coating process. These findings are consistent with the opacity results, which, although slightly increased in the parchment paper samples, did not vary significantly for polystyrene. This supports the conclusion that the applied coatings did not compromise the visual characteristics of the substrates, thereby preserving their aesthetic quality—a relevant factor for potential commercial applications.

Prior studies on biopolymer films and active packaging materials have similarly demonstrated minimal changes in optical or colorimetric parameters when bioactive agents are incorporated; for example, nanofibers based on HPMC blends have been shown to form uniform fibrous mats and exhibit favorable physicochemical characteristics (Aydogdu et al., 2018). In HPMC-based films, transparency and gloss (closely related to opacity) were maintained after the addition of surfactants, indicating minimal impact on visual appearance (Cabrera-Barjas et al., 2025). A review of electrospun nanofiber systems for food packaging also highlights that optical and visual properties are a key concern when embedding active agents in fibrous matrices (Yang et al., 2025).

Surface Hydrophobicity and Water Vapor Permeability To evaluate the moisture interaction of the samples after coating, water contact angles were measured (Table 3).

As shown in Table 3, uncoated parchment paper (control) exhibited a high contact angle of 107.55°, which characterizes a highly hydrophobic surface, likely due to its intrinsic surface roughness. Upon application of the coating, both with and without phages, a significant reduction in contact angle was observed, indicating a clear decrease in surface hydrophobicity. This effect is attributed to the hydrophilic nature of the sodium alginate and HPMC blend used in the formulation, which increases the wettability of the surface by facilitating the spreading of water droplets.

A similar trend was noted for polystyrene substrates, which initially presented a moderately hydrophobic profile. After coating, the contact angles also decreased, reinforcing the role of the alginate-HPMC mixture in enhancing surface hydrophilicity regardless of the substrate. These results confirm that the application of the phage-containing or phage-free coating effectively alters the surface properties by promoting hydrophilicity.

Table 3 Contact angle (°) and WVTR (g/m^2 day) values for the different material matrices

Matrix		Contact angle (°)	WVTR (g/m^2 day)
Parchment paper	Control	107.55 ± 7.85^{A}	233.31 ± 4.46^{A}
	Without phages	48.35 ± 1.76^{B}	235.56 ± 6.16^{A}
	With phages	45.70 ± 0.70^{B}	238.26 ± 4.01^{A}
Polystyrene	Control	91.45 ± 0.21^{A}	14.61 ± 0.13^{A}
	Without phages	74.10 ± 2.68^{B}	14.81 ± 0.58^{A}
	With phages	70.05 ± 7.42^{B}	14.80 ± 0.07^{A}

Superscript letters (A, B): Within each respective material group, values in the same column not sharing upper case superscript letters indicate statistically significant differences between each other ($p < 0.05$).

Table 4 Tensile strength (TS), elongation at break (EB), and Young's modulus (YM) values for the different material matrices

Matrix		TS (MPa)	EB (%)	YM (MPa)
Parchment paper	Control	34.45 ± 4.09^{A}	6.39 ± 2.44^{A}	1602.87 ± 19.38^{A}
	Without phages	55.53 ± 3.27^{B}	5.60 ± 3.35^{A}	3765.75 ± 24.64^{B}
	With phages	60.20 ± 9.20^{B}	5.02 ± 2.73^{A}	3766.88 ± 28.87^{B}
Polystyrene	Control	46.08 ± 5.92^{A}	31.53 ± 1.61^{A}	1946.59 ± 17.59^{A}
	Without phages	45.26 ± 2.70^{A}	28.18 ± 0.66^{A}	2093.61 ± 22.31^{A}
	With phages	46.62 ± 4.02^{A}	27.90 ± 9.14^{A}	2004.86 ± 13.53^{A}

Superscript letters (A, B): Within each respective material group, values in the same column not sharing upper case superscript letters indicate statistically significant differences between each other ($p < 0.05$).

The effectiveness of water vapor and gas barrier properties is essential for evaluating packaging materials. Control tests were performed using uncoated parchment paper and polystyrene under standardized conditions. As expected, the uncoated parchment paper exhibited a high water vapor transmission rate (WVTR), which can be attributed to its intrinsically porous structure, as confirmed by SEM analysis ("Morphology Analysis" section). This is further intensified by the hydrophilic nature of cellulose fibers, which readily absorb moisture and facilitate water vapor permeation (Li et al., 2007).

Following the application of the coating, a slight increase in WVTR was observed for both parchment paper and polystyrene substrates. This effect is likely due to the hydrophilic characteristics of sodium alginate and HPMC, which may promote greater moisture uptake and thereby allow more water vapor to diffuse through the material. However, it is important to note that the applied coating layer is extremely thin and may not be sufficient to create a continuous, dense barrier. Possible microscopic discontinuities in the coating or incomplete surface coverage could also contribute to the limited change in barrier performance.

Moreover, the inclusion of bacteriophages in the formulations did not significantly affect the WVTR values, indicating that their presence does not compromise the water vapor barrier properties of the coated materials. This consistency reinforces the feasibility of incorporating phages into bioactive packaging without negatively impacting the physical integrity of the films or coatings.

Mechanical Properties The mechanical properties of the control materials, including TS, EB, and YM were determined for all substrates (Table 4).

The mechanical properties of both parchment paper and polystyrene substrates were influenced by the application of nanofiber coatings composed of sodium alginate and HPMC. Specifically, TS increased significantly for parchment paper after coating, rising from 34.45 ± 4.09 MPa in the control to 60.20 ± 9.20 MPa with phage-containing nanofibers. This improvement was also observed without phages, indicating that the coating itself, rather than phage presence, contributed to the enhanced TS. In contrast, polystyrene showed no significant changes in TS upon coating, with values remaining around 45–46 MPa regardless of treatment.

YM, a measure of stiffness, increased markedly for parchment paper with coating, more than doubling from 1602.87 ± 19.38 MPa (control) to approximately 3766 MPa with coatings, reflecting a substantial increase in rigidity. For polystyrene, YM changes were minimal and not statistically significant, indicating that the plastic substrate's mechanical properties largely dominate and are less affected by the nanofiber coatings.

The mechanical properties of the materials increased after the addition of nanofibers composed of sodium alginate and HPMC to both parchment paper and polystyrene. However, a decrease in EB was observed in both coated substrates. For parchment paper, EB dropped from $6.39 \pm 2.44\%$ in the control to around 5%, while in polystyrene, EB decreased

slightly from 31.53 ± 1.61% to approximately 28%, although these changes were not statistically significant.

The decrease in EB in parchment paper and polystyrene substrates coated with nanofibers made of sodium alginate and HPMC can be attributed to the combination of the nanofibers' rigidity, which reduces the material's flexibility (Zhang et al., 2024). Although sodium alginate and HPMC are hydrophilic polymers, their incorporation in the coating can increase rigidity and brittleness, reducing the ability to elongate before rupture. Furthermore, interactions between the polymers and substrates may create internal stresses that hinder material deformation. Additionally, the coating thickness may also contribute to the loss of flexibility, resulting in lower EB values (Zhu, 2021). Similar trends have been observed in polymeric films reinforced with nanofillers, where improvements in tensile strength and stiffness are often accompanied by a modest reduction in elongation, highlighting the trade-off between mechanical reinforcement and flexibility in bio-based packaging materials (Ashraf et al., 2025).

In summary, the nanofiber coatings significantly enhance the mechanical strength and stiffness of parchment paper but have minimal impact on polystyrene. The decrease in flexibility is slight but consistent across substrates, suggesting that the coating introduces some embrittlement, more pronounced in the inherently less flexible parchment paper. These findings are in line with recent reports demonstrating that the inclusion of biopolymer-based nanofillers can improve physicomechanical properties of food packaging materials without compromising their overall performance (Ashraf et al., 2025).

Load Efficiency and Release Rate in Phage-Loaded Nanofibers

The incorporation of bacteriophages was successfully achieved in all tested materials, including parchment paper, polystyrene, and films. It is important to note that films were prepared solely to demonstrate differences in phage incorporation and release rate and were not characterized further, as the primary focus of this study was on nanofiber-based coatings.

Despite successful phage incorporation across materials, quantitative differences were observed. All samples were prepared using the same phage solution, with a concentration of approximately 10^{10} PFU/mL, and the same volume of solution was used for both coatings and films to ensure comparability. In parchment paper, phage incorporation reached around 10^{9} PFU/mL, while polystyrene incorporated approximately 10^{8} PFU/mL. This reduced incorporation in polystyrene can be attributed to a lower amount of nanofiber deposited on its surface, which was confirmed by thickness measurements: parchment paper coatings reached nearly 5 µm, whereas polystyrene coatings exhibited a significantly lower thickness of around 2 µm. This suggests a reduced deposition of nanofibers on polystyrene, likely due to its lower surface energy, which weakens the interaction with the hydrophilic nanofiber components, limiting adhesion and accumulation—an effect also reported by Choi et al. (2017).

The phage release profile was assessed across materials to evaluate the differences in release kinetics (Fig. 3B). Although phages were released from all matrices, the kinetics varied. Films and parchment paper coatings released nearly 100% of incorporated phages, while polystyrene coatings reached 93.46%. In all nanofiber-based samples, an initial burst release occurred, followed by rapid stabilization. Contrary to what might be expected from a truly controlled release system, phage release was completed within a short time frame—approximately 20 min for films and parchment paper coatings, and around 40 min for polystyrene. Therefore, the system does not exhibit sustained or prolonged release, but rather a fast diffusion of phages likely driven by the hydrophilic and porous nature of the nanofibers.

This behavior is consistent with literature findings. For example, Korehei and Kadla (2014) showed that T4 phages encapsulated in electrospun fibers of PEO and CDA exhibited delayed release due to increased fiber diameter. Similarly, Costa et al. (2018) reported that phage Felix O1 encapsulated in nanofiber-based films displayed distinct thermal behavior compared to conventional films, reinforcing the functional differences introduced by nanostructured coatings.

Altogether, these results demonstrate the feasibility of incorporating and rapidly releasing bacteriophages from nanofiber coatings, with variations in performance depending on substrate properties. Although release is not prolonged, this rapid delivery may still be beneficial for food packaging applications requiring immediate antimicrobial action upon contact with contaminated surfaces.

In addition to release behavior, the potential safety of the developed materials was also considered, given their intended application in food packaging. Bacteriophages are generally recognized as safe (GRAS) and have been widely reported as non-toxic to humans (Narayanan et al., 2024); however, aspects such as stability, migration, and unintended release must still be addressed. In our system, the rapid release profile limits prolonged exposure of phages to the packaging matrix, reducing the likelihood of structural degradation or formation of harmful by-products. The hydrophilic polymers used (sodium alginate and HPMC) are food-grade and approved for packaging applications, further supporting safety. While some migration of phages to the food surface is expected and desired for antimicrobial action, the materials do not promote uncontrolled or sustained release.

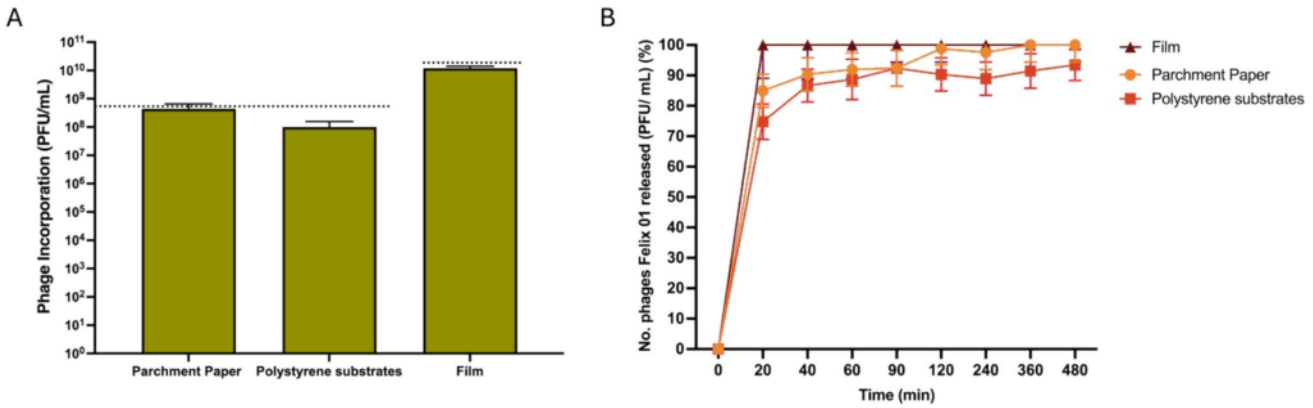

Fig. 3 Phage loading and release profile from nanofiber-coated substrates. **A** Phage incorporation expressed as PFU/mL quantified after nanofiber deposition on parchment paper, polystyrene, and film. **B** Temporal profile of phage release from the different substrates over time

Table 5 Antibacterial efficacy of different material matrices with *Salmonella* phages

Matrix		Antibacterial activity (*A*)	Efficacy of antibacterial property
Salmonella phages	Film	2.93	Significant
	Parchment paper	2.05	Significant
	Polystyrene substrates	0.76	Low

Antimicrobial Activity of Phage-Loaded Nanofibers

The antibacterial activity of the samples was evaluated following the ISO 22196 standard (Table 5). According to this standard, antibacterial activity (A) is classified as follows: $A < 2$ indicates low antibacterial efficacy, $2 \leq A < 3$ indicates significant efficacy, and $A \geq 3$ denotes strong antibacterial efficacy.

The samples demonstrated significant antibacterial activity against *Salmonella* in film samples and coated parchment paper substrates, while coated polystyrene substrates exhibited low antibacterial activity (Table 5). This difference in activity is likely attributed to the lower deposition of nanofibers in the polystyrene coating layer, which had only 3.75% coating compared to 15.75% in parchment paper, and consequently a lower concentration of phages in the tested sample as shown in Fig. 3.

The antimicrobial effectiveness of the phage-loaded coatings and films against *Salmonella* was confirmed by the formation of clear inhibition zones on agar plates after incubation (Fig. 4). After 24 and 72 h of incubation at 30 °C and 37 °C, all phage-containing materials exhibited halos, confirming that active bacteriophages remained functional and were able to inhibit bacterial growth.

According to the results obtained (Table 6), the strongest inhibition was recorded for films, with halo diameters of 24 mm after 24 h and 25 mm after 72 h. Coated parchment paper and polystyrene substrates both exhibited inhibition zones of 16–17 mm, with no substantial increase over time. These results support the superior antibacterial performance of the films, which can be attributed to their higher phage concentration and more uniform phage distribution across the surface. As previously discussed, films incorporated approximately 10^{10} PFU/mL of phages, while parchment paper and polystyrene coatings incorporated around 10^{9} and 10^{8} PFU/mL, respectively. This difference in loading likely provides films with a greater reservoir of phages that can be released over time, sustaining antibacterial activity and potentially extending the functional lifespan of the coating.

Despite the differences in incorporation levels, parchment paper and polystyrene coatings demonstrated similar inhibition halo diameters. This apparent discrepancy may be explained by two complementary mechanisms. First, both coatings likely undergo a burst release of phages immediately upon contact with the assay medium, delivering a high concentration of bioactive phages sufficient to inhibit bacterial growth within the first 24 h. This rapid initial release may overshadow differences in total phage loading, leading to comparable inhibition zones (Ali et al., 2025). Second, the halo assay itself may reach a saturation point, wherein the measured inhibition zone no longer scales proportionally with surface phage concentration once a threshold sufficient for bacterial inhibition is exceeded (Chevallier et al., 2023). Together, these factors suggest that while phage

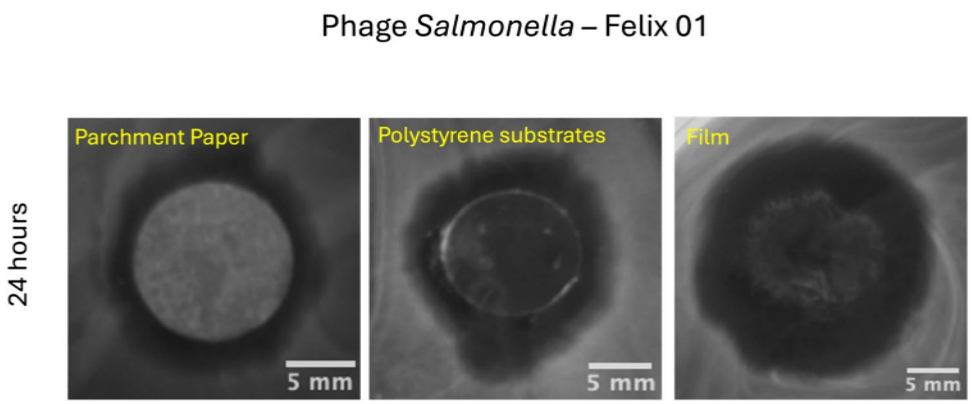

Fig. 4 Antimicrobial activity of phage-incorporated sodium alginate and HPMC-based films and coatings against *Salmonella*. The images show inhibition zones formed by phage-treated films, tracing paper, and polystyrene substrates after 24 h of incubation

Table 6 Inhibition halo diameters (mm) observed for sodium alginate and HPMC-based films and coatings incorporated with phages against *Salmonella* after 24 and 72 h of incubation

Matrix		Halo diameters	
		24 h	72 h
Salmonella phages	Parchment paper	16 mm	17 mm
	Polystyrene substrates	17 mm	17 mm
	Film	24 mm	25 mm

incorporation levels influence long-term antibacterial performance, short-term assays such as the halo test primarily reflect the initial bioavailability of phages and may not capture subtle differences in loading between substrates.

These findings are in line with other studies that have demonstrated the antimicrobial potential of phage-loaded nanofibers. For instance, Kielholz et al. (2023) reported that electrospun fiber mats incorporating bacteriophages produced larger inhibition zones (8.4–8.7 mm) compared to phage lysates or lysate-impregnated disks, indicating improved bioavailability and stability of the phages when embedded in nanofibers. Similarly, Suchithra et al. (2025) showed that nanofiber matrices loaded with dual phages exhibited superior antimicrobial activity against Pseudomonas aeruginosa and Staphylococcus aureus, with clearer and more defined inhibition zones than free phage solutions, suggesting that the nanofiber structure offers protection and possibly enhances release kinetics.

Overall, the incorporation of phages into electrospun nanofiber coatings shows promising antibacterial activity, even though films achieve stronger inhibition due to higher phage loading. The comparable results between parchment paper and polystyrene coatings suggest that, despite differing levels of nanofiber deposition and surface interaction, both substrates can effectively deliver phages in concentrations sufficient to inhibit *Salmonella* growth in vitro.

Taken together, these results demonstrate that electrospun phage-loaded coatings are capable of delivering effective antimicrobial activity across different substrates, even when phage loading varies. Beyond their biological performance, it is also important to consider whether such coatings are feasible for industrial implementation. The materials used in this work—sodium alginate, HPMC, and bacteriophages—are low-cost, commercially available, and already employed in food-related applications, which supports their potential scalability. Moreover, electrospinning technology has advanced toward continuous roll-to-roll systems, which significantly reduces production time and enables uniform deposition on large packaging surfaces. Phage production itself is inexpensive and can be scaled to high titers using standard fermentation and purification workflows. Because the coatings applied here require only thin nanofiber layers, material consumption remains low, helping maintain economically viable production costs. Therefore, considering material affordability, processing scalability, and the minimal amount of polymer and phage required, the proposed nanofiber-based approach appears realistic for industrial-scale adoption, particularly for high-value foods where enhanced microbial safety is critical.

Conclusions

This study successfully demonstrated the development and application of dual-polymer electrospun nanofibers incorporating bacteriophages into sodium alginate and HPMC matrices, directly deposited onto real food-grade packaging materials (parchment paper and polystyrene). This approach offers a practical and scalable pathway for the integration of phage-based antimicrobial functionality into packaging systems. Nanofiber deposition was more efficient on parchment paper (thickness ≈ 46.5 µm; grammage 0.58 g/m^2) than on polystyrene (thickness ≈ 59.7 µm; grammage 0.21 g/m^2), resulting in higher phage incorporation (≈10^9 PFU/mL vs. ≈10^8 PFU/mL) and improved antibacterial activity. Surface characterization confirmed increased hydrophilicity after coating, particularly in

parchment paper, whose contact angle decreased from 107.6 to 45.7°, while water vapor permeability remained largely unaffected, indicating that the thin nanofiber layer does not compromise barrier performance.

Phage release exhibited a burst-release profile across all materials, with films and parchment coatings releasing nearly 100% of loaded phages within ~ 20 min, whereas polystyrene released 93.5% within ~ 40 min. Antibacterial activity correlated directly with phage loading: films showed the largest inhibition halos (24–25 mm), followed by parchment coatings (16–17 mm), and polystyrene coatings, which exhibited the lowest activity due to reduced nanofiber deposition (3.75% coverage vs. 15.75% on parchment). These results demonstrate that substrate surface properties play a central role in determining coating adhesion, phage incorporation, and overall antimicrobial performance.

Beyond confirming the effectiveness of phage-loaded nanofibers for pathogen control, this work advances the field by showing through a systematic, quantitative evaluation that a dual-polymer hydrophilic matrix can be successfully electrospun onto commercially relevant packaging materials while maintaining phage viability and functionality. This represents a notable departure from previous phage-electrospinning studies largely limited to biomedical substrates. Importantly, the materials and processing conditions used here are compatible with scalable manufacturing, and the low cost of biopolymers and phage production enhances the industrial feasibility of this approach.

Overall, the insights gained on substrate–fiber interactions, incorporation efficiency, release kinetics, and antimicrobial performance provide a foundation for the further optimization of phage-based active packaging technologies. Future work should prioritize improving long-term phage stability and mechanical robustness to fully enable industrial adoption and maximize the potential of bacteriophage nanotechnology in enhancing food safety.

Acknowledgements Sanna Sillankorva acknowledges funding by FCT through the individual scientific employment program contract (2020.03171.CEECIND). Victor G.L. de Souza acknowledges FCT/MECI for funding his individual contract (https://doi.org/10.54499/2023.09446.CEECIND/CP2836/CT0011).

Author Contribution Fernanda Coelho: Writing – review & editing, Methodology, Investigation; Pedro Miguel Silva: Writing – review & editing, Methodology, Investigation; Victor Gomes Lauriano de Souza: Writing – review & editing, Methodology, Investigation; Lorenzo Pastrana: Supervision, Resources, Funding acquisition; Sanna Sillankorva: Supervision, Writing – review & editing, Methodology, Investigation Valtencir Zucolloto: Supervision, Resources, Funding acquisition.

Funding The Article Processing Charge (APC) for the publication of this research was funded by the Coordenação de Aperfeiçoamento de Pessoal de Nível Superior - Brasil (CAPES) (ROR identifier: 00x0ma614). The authors acknowledge financial support from the FAPESP (Grant No. 2023/14222–7).

Data Availability No datasets were generated or analysed during the current study.

Declarations

Competing Interests The authors declare no competing interests.

References

Adams, M. H. (1959). *Bacteriophages*. Interscience Publishers. https://doi.org/10.1002/ange.19620740437

Ali, H. R., Valdivia, C., & Negus, D. (2025). Bacteriophage-embedded and coated alginate layers inhibit biofilm formation by clinical strains of Klebsiella pneumoniae. *Journal of Applied Microbiology, 136*, 5. https://doi.org/10.1093/jambio/lxaf099

Alves, D., Marques, A., Milho, C., Costa, M. J., Pastrana, L. M., Cerqueira, M. A., et al. (2019). Bacteriophage ϕIBB-PF7A loaded on sodium alginate-based films to prevent microbial meat spoilage. *International Journal of Food Microbiology, 291*, 121–127. https://doi.org/10.1016/j.ijfoodmicro.2018.11.026

American Society for Testing and Materials (ASTM). (2010). *ASTM D882-10: Standard test method for tensile properties of thin plastic sheeting*. ASTM International. https://www.astm.org/d0882-10.html

American Society for Testing and Materials (ASTM). (2007). *ASTM D646-96: Standard test method for grammage of paper and paperboard (mass per unit area)*. ASTM International. https://www.astm.org/d0646-96.html

American Society for Testing and Materials (ASTM). (2013). *ASTM E96/E96M-13: Standard test methods for water vapor transmission of materials*. ASTM International. https://www.astm.org/e0096-13.html

Ashraf, J., Ismail, N., Tufail, T., Zhang, J., Chen, J., Rehman, A., Ahmed, Z., & Xu, B. (2025). Technological advancements in zein-based nano-colloids: Current emerging trends in sustainable packaging and their potential in enhancing shelf-life of fresh fruits. *Food Packaging and Shelf Life, 49*, Article 101523. https://doi.org/10.1016/j.fpsl.2025.101523

Aydogdu, A., Sumnu, G., & Sahin, S. (2018). A novel electrospun hydroxypropyl methylcellulose/polyethylene oxide blend nanofibers: Morphology and physicochemical properties. *Carbohydrate Polymers, 181*, 234–246. https://doi.org/10.1016/j.carbpol.2017.10.071

Becerril, R., Nerín, C., & Silva, F. (2020). Encapsulation systems for antimicrobial food packaging components: An update. *Molecules, 25*(5), Article 1134. https://doi.org/10.3390/molecules25051134

Blachowicz, T., & Ehrmann, A. (2023). Optical properties of electrospun nanofiber mats. *Membranes, 13*(4), Article 441. https://doi.org/10.3390/membranes13040441

Cabrera-Barjas, G., González, M., Benavides-Valenzuela, S., Preza, X., Paredes-Padilla, Y. A., Castaño-Rivera, P., Segura, R., Durán-Lara, E. F., & Nesic, A. (2025). Active packaging based on hydroxypropyl methyl cellulose/fungal chitin nanofibers films for controlled release of ferulic acid. *Polymers, 17*, Article 2113. https://doi.org/10.3390/polym17152113

Centers for Disease Control and Prevention (CDC, 2023). Available online: https://www.cdc.gov/salmonella/index.html (accessed on 11 march 2025).

Chevallier, P., Wiggers, H. J., Copes, F., Zorzi Bueno, C., & Mantovani, D. (2023). Prolonged antibacterial activity in tannic acid-iron complexed chitosan films for medical device applications. *Nanomaterials (Basel), 13*(3), Article 484. https://doi.org/10.3390/nano13030484

Choi, W., Kim, G. H., Shin, J. H., Lim, G., & An, T. (2017). Electrospinning onto insulating substrates by controlling surface wettability and humidity. *Nanoscale Research Letters, 12*, Article 610.2017. https://doi.org/10.1186/s11671-017-2380-6

Coelho, F., de Souza, V. G. L., Pastrana, L., et al. (2025). Phage-enhanced materials: Antimicrobial films and coatings targeting *Pseudomonas fluorescens* and *Escherichia coli*. *Food and Bioprocess Technology, 18*, 9821–9837. https://doi.org/10.1007/s11947-025-03996-2

Costa M. J., Catarina Milho J. A. T., Sillankorva S., Cerqueira M. A., and Loyd K. N., (2018). Electrospun nanofibres as a novel encapsulation vehicle for Felix O1 bacteriophage for new food packaging applications. IUFoST 2018 - World Congress of Food Science and Technology. No. 755, Mumbai, India, Oct 23–27, 554.

Costa, M. J., Pastrana, L. M., Teixeira, J. A., Sillankorva, S., & Cerqueira, M. A. (2021). Characterization of PHBV films loaded with FO1 bacteriophage using polyvinyl alcohol-based nanofibers and coatings: A comparative study. *Innovative Food Science & Emerging Technologies, 69*, Article 102646. https://doi.org/10.1016/j.ifset.2021.102646

Espitia, P. J. P., Avena-Bustillos, R. J., Du, W. X., Teófilo, R. F., Soares, N. F., & McHugh, T. H. (2014). Optimal antimicrobial formulation and physical-mechanical properties of edible films based on açaí and pectin for food preservation. *Food Packaging and Shelf Life, 2*, 38–49. https://doi.org/10.1016/j.fpsl.2014.06.002

European Food Safety Authority (EFSA) 2024. Available online: https://www.efsa.europa.eu/en (accessed on 11 march 2025).

Ghaani, M., Cozzolino, C. A., Castelli, G., & Farris, S. (2016). An overview of the intelligent packaging technologies in the food sector. *Trends in Food Science & Technology, 51*, 1–11. https://doi.org/10.1016/j.tifs.2016.02.008

Greiner, A., & Wendorff, J. H. (2007). Electrospinning: A fascinating method for the preparation of ultrathin fibers. *Angewandte Chemie International Edition, 46*, 5670–5703. https://doi.org/10.1002/anie.200604646

Huang, K., & Nitin, N. (2019). Edible bacteriophage based antimicrobial coating on fish feed for enhanced treatment of bacterial infections in aquaculture industry. *Aquaculture, 502*, 18–25. https://doi.org/10.1016/j.aquaculture.2018.12.026

Kielholz, T., Rohde, F., Jung, N., & Windbergs, M. (2023). Bacteriophage-loaded functional nanofibers for treatment of *P. aeruginosa* and *S. aureus* wound infections. *Scientific Reports, 13*, Article 8330. https://doi.org/10.1038/s41598-023-35364-5

Korehei, R., & Kadla, J. F. (2014). Encapsulation of T4 bacteriophage in electrospun poly(ethylene oxide)/cellulose diacetate fibers. *Carbohydrate Polymers, 100*, 150–157. https://doi.org/10.1016/j.carbpol.2013.03.079

Li, X., Tabil, L. G., & Panigrahi, S. (2007). Chemical treatments of natural fiber for use in natural fiber-reinforced composites: A review. *Journal of Polymers and the Environment, 15*, 25–33. https://doi.org/10.1007/s10924-006-0042-3

Marangoni Júnior, L., Rodrigues, P. R., Silva, R. G., Vieira, R. P., & Alves, R. M. V. (2021). Sustainable packaging films composed of sodium alginate and hydrolyzed collagen: Preparation and characterization. *Food and Bioprocess Technology, 14*, 2336–2346. https://doi.org/10.1007/s11947-021-02727-7

Mathew, M., Paroly, S., & Athiyanathil, S. (2025). Biopolymer-based electrospun nanofiber membranes for smart food packaging applications: A review. *RSC Advances, 27*, 2025. https://doi.org/10.1039/D5RA02348C

Narayanan, K. B., Bhaskar, R., & Han, S. S. (2024). Bacteriophages: Natural antimicrobial bioadditives for food preservation in active packaging. *International Journal of Biological Macromolecules, 276*, Article 133945. https://doi.org/10.1016/j.ijbiomac.2024.133945

Sambrook, J., & Russell, D. W. (2001). *Molecular cloning: A laboratory manual* (3rd Edition, Vol. 1). Cold Spring Harbor Laboratory Press.

Samyn, P. (2013). Wetting and hydrophobic modification of cellulose surfaces for paper applications. *Journal of Materials Science, 48*, 6455–6498. https://doi.org/10.1007/s10853-013-7519-y

Suchithra, K. V. S., Hameed, A., Surya, S., Mahammad, S., & Arun, A. B. (2025). Dual phage-incorporated electrospun polyvinyl alcohol-eudragit nanofiber matrix for rapid healing of diabetic wound infected by *Pseudomonas aeruginosa* and *Staphylococcus aureus*. *Drug Delivery and Translational Research, 15*, 1092–1108. https://doi.org/10.1007/s13346-024-01660-4

Wagh, R. V., Priyadarshi, R., & Rhim, J.-W. (2023). Novel bacteriophage-based food packaging: An innovative food safety approach. *Coatings, 13*, Article 609. https://doi.org/10.3390/coatings13030609

Xie, J., Yang, F., Shi, H., Yan, J., Shen, H., Yu, S., Gan, N., Feng, B., & Wang, L. (2022). Protein FT-IR amide bands are beneficial to bacterial typing. *International Journal of Biological Macromolecules, 207*, 358–364. https://doi.org/10.1016/j.ijbiomac.2022.02.161

Xue, J., Wu, T., Dai, Y., & Xia, Y. (2019). Electrospinning and electrospun nanofibers: Methods, materials, and applications. *Chemical Reviews, 119*(8), 5298–5415. https://doi.org/10.1021/acs.chemrev.8b00593

Yang, J., Wang, H., Lou, L., & Meng, Z. (2025). A review of chitosan-based electrospun nanofibers for food packaging: From fabrication to function and modeling insights. *Nanomaterials, 15*(16), Article 1274. https://doi.org/10.3390/nano15161274

Zanetti, M., Carniel, T. K., Dalcanton, F., Anjos, R. S., Riella, H. G., Araújo, P. H. H., Oliveira, D., & Fiori, M. A. (2018). Use of encapsulated natural compounds as antimicrobial additives in food packaging: A brief review. *Trends in Food Science & Technology, 81*, 51–60. https://doi.org/10.1016/j.tifs.2018.09.003

Zhang, M., Ahmed, A., & Xu, L. (2023). Electrospun nanofibers for functional food packaging application. *Materials, 16*, 5937. https://doi.org/10.3390/ma16175937

Zhang, Z., Liu, H., Yu, D. G., & Bligh, S.-W. (2024). Alginate-based electrospun nanofibers and the enabled drug controlled release profiles: A review. *Biomolecules, 14*(7), Article 789. https://doi.org/10.3390/biom14070789

Zhu, F. (2021). Polysaccharide based films and coatings for food packaging: Effect of added polyphenols. *Food Chemistry, 359*, Article 129871. https://doi.org/10.1016/j.foodchem.2021.129871